Washington University School of Medicine
Digital Commons@Becker

Open Access Publications

2017

Linear ion-trap MSn with high-resolution MS reveals structural diversity of 1-O-acylceramide family in mouse epidermis

Meei-Hua Lin
Washington University School of Medicine in St. Louis

Jeffrey H. Miner
Washington University School of Medicine in St. Louis

John Turk
Washington University School of Medicine in St. Louis

Fong-Fu Hsu
Washington University School of Medicine in St. Louis

Follow this and additional works at: https://digitalcommons.wustl.edu/open_access_pubs

Recommended Citation

methods

Linear ion-trap MS^n with high-resolution MS reveals structural diversity of 1-O-acylceramide family in mouse epidermis[s]

Meei-Hua Lin,* Jeffrey H. Miner,* John Turk,[†] and Fong-Fu Hsu[1,†]

Division of Nephrology* and Mass Spectrometry Resource, Division of Endocrinology, Diabetes, Metabolism, and Lipid Research,[†] Department of Medicine, Washington University School of Medicine, St. Louis, MO

Abstract 1-O-acylceramide is a new class of epidermal ceramide (Cer) found in humans and mice. Here, we report an ESI linear ion-trap (LIT) multiple-stage MS (MS^n) approach with high resolution toward structural characterization of this lipid family isolated from mice. Molecular species desorbed as the $[M + H]^+$ ions were subjected to LIT MS^2 to yield predominately the $[M + H - H_2O]^+$ ions, followed by MS^3 to cleave the 1-O-acyl residue to yield the $[M + H - H_2O - (1\text{-}O\text{-}FA)]^+$ ions. The structures of the N-acyl chain and long-chain base (LCB) of the molecule were determined by MS^4 on $[M + H - H_2O - (1\text{-}O\text{-}FA)]^+$ ions that yielded multiple sets of specific ions. Using this approach, isomers varied in the 1-O-acyl (from 14:0- to 30:0-O-acyl) and N-acyl chains (from 14:0- to 34:1-N-acyl) with 18:1-sphingosine as the major LCB were found for the entire family. Minor isomers consisting of 16:1-, 17:1-, 18:2-, and 19:1-sphingosine LCBs with odd fatty acyl chain or with monounsaturated N- or O-fatty acyl substituents were also identified. An estimation of more than 700 1-O-acylceramide species, largely isobaric isomers, are present, underscoring the complexity of this Cer family.—Lin, M-H., J. H. Miner, J. Turk, and F-F. Hsu. Linear ion-trap MS^n with high-resolution MS reveals structural diversity of 1-O-acylceramide family in mouse epidermis. *J. Lipid Res.* 2017. **58:** 772–782.

The outermost layer of the epidermis in mammals is rich in ceramides (Cers), which provide a physical barrier to water loss and proper skin functions (1–3). Epidermal Cers are mainly found in extracellular lipid lamellae and contain various classes of Cers, including those having unusual long-chain amide-linked ω-hydroxyacids, to which the ω-hydroxy group is esterified with an additional long-chain FA, primarily a linoleic acid (4–6).

In addition to the esterified ω-hydroxy FA-containing Cer class, Cers consisting of long to very long N- and 1-O-linked acyl chains were recently identified in humans and mice. This new class of epidermal 1-O-acylceramide derives from classical group I amide-linked nonhydroxy sphingosine Cers and makes up 5% of all esterified Cers. They are hydrophobic and were thought to contribute to the water barrier homeostasis (7).

A large body of literature on the quantitative and qualitative analysis of Cers using mass spectrometric techniques, including GC/MS (8, 9) and ESI tandem MS with or without online HPLC (10–18), has been published; however, very few studies have focused on the structural characterization of complex skin Cers. Among them, Masukawa et al. (15) and t'Kindt et al. (16) conducted the most extensive LC/MS/MS analysis of Cers in human stratum corneum, and revealed hundreds of Cer species in various classes, including many isobaric isomers, but species in the 1-O-acylceramide family were not reported. Rabionet et al. (7) reported the presence of 1-O-acylceramides and a minor 1-O-acylceramide subfamily comprising the N-α-hydroxyacyl group in human and mouse epidermis using UPLC-ESI-tandem quadrupole MS and several isobaric isomers were found. Here, we apply linear ion-trap (LIT) multiple-stage MS (MS^n) in combination with high-resolution accurate mass measurements to unveil the structural details of the 1-O-acylceramides isolated from mouse epidermis. Our results reveal the complexity of this 1-O-acylceramide

Abbreviations: AMPP, N-(4-aminomethylphenyl) pyridinium; Cer, ceramide; CID, collision-induced dissociation; FATP4, FA transport protein 4; HCD, higher collision energy dissociation; LCB, long-chain base; LIT, linear ion-trap; MS^n, multiple-stage MS.

[1]To whom the correspondence should be addressed.
e-mail: fhsu@im.wustl.edu
[s] The online version of this article (available at http://www.jlr.org) contains a supplement.

family, which consists of C_{18}-sphingosine as the major long-chain base (LCB) together with minor C_{16}-, C_{17}-, C_{18}-, C_{19}-, and C_{20}-sphingosine LCBs and a C_{18}-dehydrosphingosine LCB to which a whole array of amide-linked fatty acyl substituents (ranging from C_{14} to C_{32} with zero to one double bond) and 1-O-linked acyl groups (ranging from C_{14} to C_{32} with zero to one double bond) are attached.

MATERIALS AND METHODS

Chemicals

All chemicals and solvents were purchased from Fisher Scientific (Waltham, MA). Standard 1-O-oleoyl-N-heptadecanoyl-D-erythro-sphingosine (18:1-d18:1/17:0-Cer; please refer to the Nomenclature section for an explanation of abbreviations such as this) was purchased from Avanti Polar Lipids, Inc. (Alabaster, AL). An AMP+ MS kit (50 test) containing N-(4-aminomethylphenyl) pyridinium (AMPP) derivatizing reagent, n-butanol (HOBt), 1-ethyl-3-(3-dimethylaminopropyl)carbodiimide, and acetonitrile/DMF solution was purchased from Cayman Chemical (Ann Arbor, MI).

Preparation and isolation of 1-O-acylceramides from mouse epidermis

To the lyophilized 10 mg epidermis sample from newborn mice in a centrifuge tube, 0.8 ml water was added. The sample was soaked for 5 min at room temperature and 3 ml chloroform/methanol (1:2, v:v) were added. Following 30 s vortexing and 2 h shaking at room temperature, an additional 1 ml chloroform and 1 ml water were added. The extraction tube was vortexed for another 30 s, centrifuged at $1750 \times g$ at room temperature for 5 min, and the organic layer was transferred to another tube, dried under nitrogen, and stored at $-20°C$ until use. To fractionate, the crude lipids redissolved in 500 ul $CHCl_3$ were loaded to a 3 ml/500 mg Macherey-Nagel (Duren, Germany) amino Chromabond Sep-Pak column, which was prewashed with 2×3 ml hexane. The column was first eluted with 3 ml hexane:diethyl ether (90:10, v:v) (fraction 1), followed by 3 ml hexane:ethyl acetate (75:25, v:v) (fraction 2), 3 ml chloroform:methanol (15:1, v:v) (fraction 3), 2×3 ml diisopropyl ether:acetic acid (98:5, v:v) (fractions 4 and 5), and finally eluted with 3 ml acetone:methanol (9:1.4, v:v) (fraction 6) by gravity. The eluants containing 1-O-acylceramide (fraction 2) and minor 1-O-acyl-N-α-OH-acylceramide (fraction 3) lipids were dried under a stream of nitrogen. The dried samples were redissolved in $CHCl_3:CH_3OH$ (1:2, v:v) before ESI-MS analysis.

Preparation of FA-AMPP derivative for locating the double bonds on the FA chain

To locate the double bond along the 1-O-acyl and N-acyl chains, 1-O-acylceramide was hydrolyzed in 1 ml of solution prepared from 8.6 ml of concentrated HCl and 9.6 ml of water, diluted to 100 ml with methanol as previously described (19). After heating at 80°C for 18 h, the hydrolysate was evaporated to dryness with a stream of nitrogen, and FA-AMPP derivative was prepared with the AMP+ MS kit according to the manufacturer's instructions, as described previously (20).

MS

Both high-resolution ($R = 100,000$ at m/z 400) higher collision energy dissociation (HCD) and low-energy collision-induced dissociation (CID) tandem MS experiments were conducted on a Thermo Scientific (San Jose, CA) LTQ Orbitrap Velos mass spectrometer with an Xcalibur operating system. Lipid extracts in chloroform/methanol (2/1) were infused (1.5 μl/min) to the ESI source, where the skimmer was set at ground potential, the electrospray needle was set at 4.0 kV, and temperature of the heated capillary was 300°C. The automatic gain control of the ion trap was set to 5×10^4, with a maximum injection time of 50 ms. Helium was used as the buffer and collision gas at a pressure of 1×10^{-3} mbar (0.75 mTorr). The MS^n experiments were carried out with an optimized relative collision energy ranging from 30 to 45% with an activation q value at 0.25 and the activation time at 10 ms to leave a minimal residual abundance of precursor ion (around 20%). The mass selection window for the precursor ions was set at 1 Da wide to admit the monoisotopic ion to the ion-trap for CID for unit resolution detection in the ion-trap or high-resolution accurate mass detection in the Orbitrap mass analyzer. Mass spectra were accumulated in the profile mode, typically for 2–10 min for MS^n spectra (n = 2–4).

Nomenclature

For simplicity, 1-O-oleoyl-N-heptadecanoyl-D-erythro-sphingosine is abbreviated as 18:1-d18:1/17:0-Cer to reflect that an oleoyl (18:1) group is attached to the 1-hydroxy LCB of d18:1/17:0-Cer by an ester bond. Likewise, Cers such as 1-O-tetraeicosanoyl-N-tetraeicosenoyl-D-erythro-sphingosine and 1-O-tetraeicosanoyl-N-tetraeicosanoyl-D-erythro-dehydrosphingosine are abbreviated as 24:0-d18:1/24:1-Cer and 24:0-d18:2/24:0-Cer, respectively. The designation of the fragment ions is according to that previously described (12).

RESULTS

The fragmentation pathways of 1-O-acylceramide

When subjected to ESI in the positive-ion mode, Cers were mainly seen as the $[M + H - H_2O]^+$ ions, due to facile loss of a water molecule (10). By contrast, 1-O-acylceramide formed $[M + H]^+$ ions, attributable to the notion that the attachment of the 1-O-acyl group may have deterred the water loss process. For example, the synthetic 18:1-d18:1/17:0-Cer standard was seen at m/z 816.7, corresponding to the $[M + H]^+$ ions, which nevertheless formed the prominent ion of m/z 798.7 (**Fig. 1A**) by loss of water, when subjected to CID in an ion-trap. The water loss most likely involved the participation of the 3-hydroxy group of LCB (**Scheme 1**). The speculation was established by the findings that further dissociation of the ion of m/z 798 (816 → 798; Fig. 1B) yielded ions of m/z 516, arising from elimination of the 1-O-oleoyl group as an acid, and of m/z 264 ($e_{3b''}$), arising from further cleavage of the N-heptaoctanoyl substituent as a ketene (Scheme 1). This fragmentation process was supported by the MS^4 spectrum of the ion of m/z 516 (816 → 798 → 516; Fig. 1C), which contained prominent ions of m/z 264 ($e_{3b''}$) (Scheme 1) that are unique to Cers consisting of C_{18}-sphingosine LCB (10). The spectrum also contained the ions of m/z 294, likely arising from cleavage of the LCB to eliminate a terminally conjugated 1,3-hexadecadiene, and of m/z 270, originated from the highly conjugated ions of m/z 516 that eliminate a $C_{18}H_{30}$ residue (Scheme 1). This latter fragmentation process also led to the ions of m/z 247, representing the highly conjugated triene cations. The
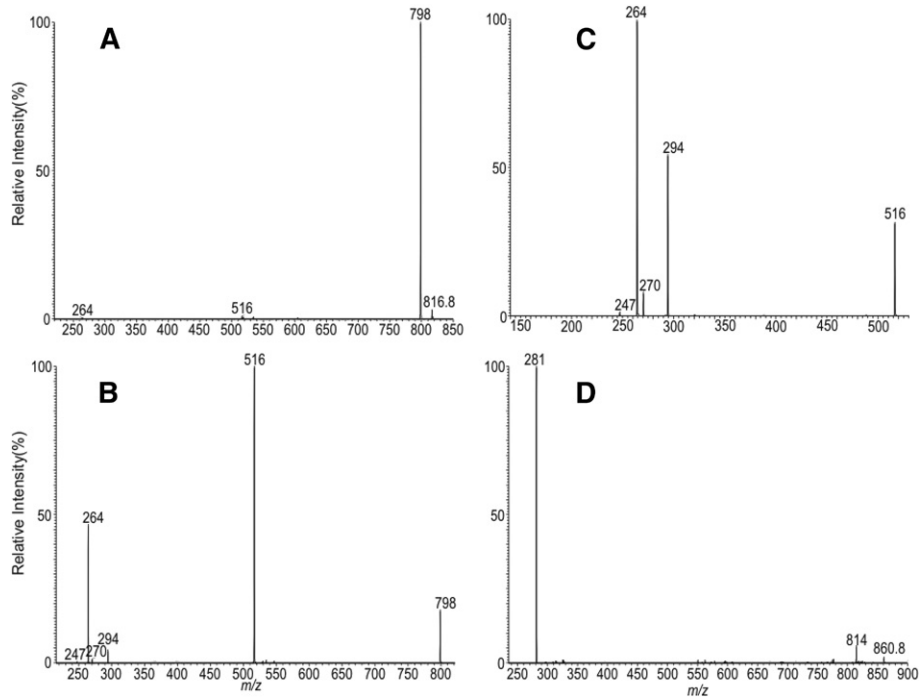
Fig. 1. The MS^2 spectrum of the $[M + H]^+$ ion of 18:1-d18:1/17:0-Cer standard at m/z 816.7 (A), its MS^3 spectrum of the ion of m/z 798.7 (816.7 → 798.7) (B), and its MS^4 spectrum of the ion of m/z 516 (816.7 → 798.7 → 516) (C). D: The MS^2 spectrum of the $[M + HCO_2]^-$ ions of 18:1-d18:1/17:0-Cer at m/z 860.8.

ions of m/z 294 and 270 are equivalent to the c_{2a} (m/z 294) and d_{1a} (m/z 270) ions, as previously described (12). The confirmation of the suggested structures is further supported by the elemental composition extracted by high-resolution MS (data not shown). The observation of the ions of m/z 264 reflecting the presence of d18:1-LCB and the 294/270 ion pair reflecting the N-heptadecanoyl substituents plus the MS^3 spectrum of m/z 798 (Fig. 1B) that defines the 1-O-oleoyl group (via loss of oleic acid) led to complete assignment of the 18:1-d18:1/17:0-Cer structure.

In the negative-ion mode in the presence of Cl^- or HCO_2^-, however, ions at m/z 850 and 860 corresponding to the $[M + Cl]^-$ and $[M + HCO_2]^-$ ions, respectively, were observed

(data not shown), similar to that previously reported for Cers (11). MS^2 on the $[M + HCO_2]^-$ ions of m/z 860 (Fig. 1D) gave prominent ions of m/z 281, corresponding to the 18:1-carboxylate anion arising from cleavage of the 1-O-fatty acyl substituent, together with the ions of m/z 814 (860 − HCO_2H) representing the $[M − H]^-$ ions arising from loss of HCO_2H. The MS^2 spectrum of the $[M + Cl]^-$ ions at m/z 850 is similar, mainly consisting of the 18:1-carboxylate anion of m/z 281 (not shown). These MS^2 spectra readily recognized the 1-O-oleoyl group, but failed to provide further structural information applicable for complete identification of the molecule and, thus, its utility in the structural identification was not investigated further.
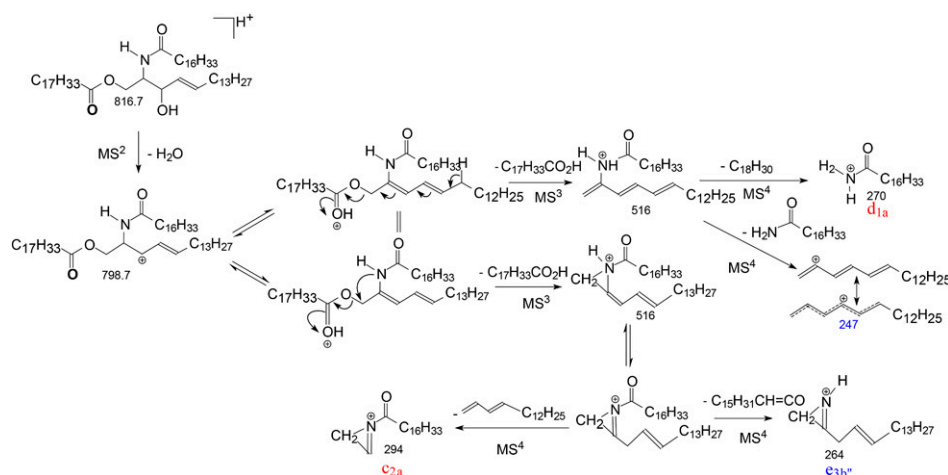
Scheme 1. The fragmentation pathways proposed for the $[M + H]^+$ ions of 1-O-oleoyl-d18:1/17:0-Cer at m/z 816.7.

Characterization of 1-O-acylceramide isolated from mouse epidermis

High-resolution ESI mass spectrometric analysis of the 1-O-acylceramides isolated from mouse epidermis (fraction 2) showed an array of abundant $[M + H]^+$ ions (**Table 1**) with an elemental composition of $C_nH_{2n-2}O_4N_1$ (n = 53–72), suggesting that the 1-O-acylceramide family mainly consists of sphingosine LCB. A minor ion series with two fewer hydrogens with an elemental composition of $C_nH_{2n-4}O_4N_1$ (n = 53–72) was also observed, indicating the presence of the minor species with an additional double bond (Table 1). The observation of the analogous of the $[M + Cl]^-$ or $[M + HCO_2]^-$ (not shown) ions in the negative ion mode is consistent with the presence of this 1-O-acylceramide family. In contrast, ions with an elemental composition of $C_nH_{2n-4}O_5N_1$ were not observed, excluding the presence of the subfamily of 1-O-acylceramides with the N-α-hydroxyacyl group previously reported by Rabionet and colleagues (6, 7) The LIT MS^n mass spectrometric approaches together with high-resolution mass measurements toward identification of these mouse epidermis 1-O-acylceramdes are described below.

Revelation of isobaric isomers in the molecular species

Multiple isobaric isomers were observed for all the ions that appeared in the ESI-MS spectrum (Table 1). For example, the MS^2 spectrum of the ions of m/z 1,001.1 is dominated by the ion of m/z 982.9 arising from loss of water (not shown). MS^3 on the ions of m/z 982.9 (1,001.1 → 982.9; **Fig. 2A**) gave rise to the prominent ions of m/z 614 arising from loss of the 1-O-24:0-FA substituent, along with minor ions at m/z 642, 628, 600, and 586 arising from losses of 1-O-22:0-, -23:0-, -25:0-, and -26:0-FA substituents, respectively. The MS^4 spectrum of m/z 614 (1,001.1 → 982.9 → 614; Fig. 2B) contained prominent ions at m/z 392 (c_{2a}) and 368 (d_{1a}) arising from cleavages of the LCB, along with the ions of m/z 264 ($e_{3b''}$), indicating the presence of the major d18:1/24:0-Cer structure (12) arising from the major 24:0-d18:1/24:0-Cer isomer. The spectrum (Fig. 2B) also contained the homologous ions at m/z 420 (c_{2a}), 396 (d_{1a}), and 236 ($e_{3b''}$) and at m/z 406 (c_{2a}), 382 (d_{1a}), and 250 ($e_{3b''}$), indicating the presence of 24:0-d16:1/26:0-Cer and 24:0-d17:1/25:0-Cer minor isomers, respectively. Similarly, the MS^4 spectrum of the ions of m/z 642 (1,001.1 → 982.9 → 642; Fig. 2C) is dominated by the ions of m/z 420 (c_{2a}), 396 (d_{1a}), and 264 ($e_{3b''}$), pointing to the presence of d18:1/26:0 structure, along with a minor ion set of m/z 434 (c_{2a}), 410 (d_{1a}), and 250 ($e_{3b''}$) that identifies the d17:1/27:0 substituent. The combined structural information from MS^3 (Fig. 2B) and MS^4 (Fig. 2C) resulted in the assignment of 22:0-d18:1/26:0- and 22:0-d17:1/27:0-Cer minor isomers. The minor isomeric LCB/N-acyl-FAs were also seen by the MS^4 spectra of the ions of m/z 628, 600, and 586 (**Table 2**) that resulted in the identification of 23:0-d17:1/26:0, 23:0-d18:1/25:0, 23:0-d16:1/27:0 (1-O-23:0 series); 25:0-d17:1/24:0, 25:0-d18:1/23:0, 25:0-d16:1/25:0 (1-O-25:0 series); and of 26:0-d16:1/24:0, 26:0-d18:1/22:0, 26:0-d17:1/23:0 (1-O-26:0 series) isobaric structures. These analyses resulted in the assignment of 14 isomers (Table 2).

Identification of 1-O-acylceramides with unsaturated bonds

In addition to the major species containing multiple isobaric isomers, minor species consisting of 1-O-acylceramides with additional double bonds located at 1-O-acyl, N-acyl substituent, or LCB are present (Table 1). For example, the MS^2 spectrum of the $[M + H]^+$ ions of m/z 998.9 is dominated by the ions of m/z 980.9 (loss of water) (data not shown) as seen earlier. MS^3 on the ions of m/z 980.9 (998.9 → 980.9; **Fig. 3A**) yielded ions at m/z 724, 698, 642, 640, 626, 614, 612, 600, and 586, arising from elimination of 1-O-16:0-, -18:1-, -22:1-, -22:0-, -23:0-, -24:1-, -24:0-, -25:1-, and -26:1-fatty acyl substituents, respectively. The MS^4 spectrum of the major ions of m/z 614 (998 → 980 → 614; data not shown) is similar to that shown in Fig. 2C, indicating that the molecules consisted of isomeric d18:1/24:0-, d16:1/26:0-, and d17:1/25:0-Cer substituents, leading to the assignment of 24:1-d18:1/24:0, 24:1-d16:1/26:0, 24:1-d17:1/25:0 isomers. MS^4 on the ions of m/z 640 (998 → 980 → 640; Fig. 3B) yielded the predominant ions of m/z 264 ($e_{3b''}$), suggesting the presence of d18:1-LCB and the $418(c_{2a})/394(d_{1a})$ ion pair that recognize the 26:1-fatty acyl substituent. The results gave assignment of the major 22:0-d18:1/26:1 isomer. The spectrum (Fig. 3B) also contained the minor ions of m/z 262 ($e_{3b''}$), which signifies the presence of d18:2-LCB, a dehydrosphingosine LCB, and the companion ions of m/z $420(c_{2a})/396(d_{1a})$ that identify the N-26:0 acyl group, indicating that a minor 22:0-d18:2/26:0-Cer isomer is also present.

Similar results were also observed for the MS^4 spectrum of the ions of m/z 612 (Fig. 3C), which is dominated by the ions of m/z 264 ($e_{3b''}$) along with the ions of m/z 390 (c_{2a}) and 366 (d_{1a}), indicating the presence of 24:0-d18:1/24:1-Cer isomer; together with ions of m/z 262 and 392/368 that identify the 24:0-d18:2/24:0 isomer; as well as the minor ion sets of m/z 236 ($e_{3b''}$) and of $418(c_{2a})/394(d_{1a})$, arising from the 24:0-d16:1/26:1 isomer, and of m/z 250 ($e_{3b''}$) and $404(c_{2a})/380(d_{1a})$ arising from the 24:0-d17:1/25:1 isomer.

The MS^4 spectra of the ions of m/z 642 (not shown) and 614 (not shown) are identical to those shown in Fig. 2, and the MS^4 spectra of the ions of m/z 626, 600, and 586 (not shown) all contain the ions that identify the LCB and N-acyl substituents of the molecules (supplemental Table S1). The combined information arising from MS^2, MS^3, and MS^4 revealed the presence of 24 isobaric structures (see supplemental Table S1).

Identification of minor 1-O-acylceramide species in the mixture

The number of the isobaric isomers appears to grow even bigger for the minor ion species, similar to those seen for other lipid classes (21). For example, the MS^2 spectrum of the ion of m/z 888.9 (data not shown) is dominated by the ion of m/z 870 (loss of water), which gives rise to the MS^3 spectrum (888 → 870; **Fig. 4A**) consisting of ions of m/z 642, 628, 614, 600, 586, 558, 530, 516, 502, 488, and 474 arising from losses of the 1-O-linked 14:0-, 15:0-, 16:0-, 17:0-, 18:0-, 20:0-, 22:0-, 23:0-, 24:0-, 25:0-, and 26:0-FA

TABLE 1. The structures of epidermal 1-O-acylceratnide revealed by LIT MS^n and high-resolution MS

m/z [M + H]$^+$	Theoretical Mass (Da)	Deviation (mDa)	Composition	Relative Intensity(%)	Major Structure	1-O-Acyl Substituent[a] Major	1-O-Acyl Substituent[a] Minor	Isomer Number
816.7804	816.7803	0.05	C53 H102 04 N		18:1-d18:1/17:0 (synthetic standard)	18:1	—	—
832.8116	832.8116	0.01	C54 H106 04 N	2.23	18:0-d18:1/18:0; 19:0-d18:1/17:0	18:0; 19:0	16:0	7
860.8431	860.8429	0.16	C56 H110 04 N	4.24	16:0-d18:1/22:0; 22:0-d18:1/16:0	16:0; 22:0	24:0; 14:0; 15:0; 20:0; 19:0; 23:0; 18:0	26
874.8586	874.8586	−0.04	C57 H112 04 N	10.50	24:0-d17:1/16:0; 16:0-d17:1/24:0	24:0; 16:0	15:0; 23:0; 14:0; 22:0; 18:0; 17:0; 25:0; 21:0	27
886.8585	886.8586	−0.12	C58 H112 04 N	2.95	24:0-d18:1/16:1; 16:0-d18:1/24:1	24:0; 16:0	22:0; 18:0; 23:1; 24:1; 25:0; 20:0; 17:0;	16
888.8742	888.8742	0.01	C58 H114 04 N	35.60	16:0-d18:1/24:0	16:0;	18:0; 24:0; 22:0 14:0; 20:0; 23:0; 15:0; 17:0; 26:0.	26
900.8739	900.8742	−0.33	C59 H114 04 N	3.32	24:0-d17:1/18:1	24:0;	18:1; 16:1; 23:0; 19:0; 25:0; 25:1; 17:1; 15:0; 22:0; 26:0;	21
902.8899	902.8899	0.03	C59 H116 04 N	21.80	18:0-d18:1/23:0; 18:0-d16:1/25:0; 16:0-d17:1/26:0	18:0; 16:0	17:0; 24:0; 15:0; 22:0; 23:0; 25:0; 20:0; 19:0; 21:0; 14:0	33
904.8688[b]	904.8692	−0.39	C58 H114 05 N	detected	24:0-d18:1/h16:0	24:0	—	1
912.8750	912.8749	0.01	C60 H114 04 N	4.33	24:0-d18:1/18:2	24:0;	18:2; 18:1; 24:1; 14:0; 16:1; 25:0; 26:0;	15
914.8900	914.8899	0.14	C60 H116 04 N	8.98	24:0-d18:1/18:1	24:0;	18:1; 16:1; 16:0; 18:0; 25:0; 26:0; 23:0;	17
916.9055	916.9055	−0.04	C60 H118 04 N	44.75	18:0-d18:1/24:0; 16:0-d18:1/26:0	18:0; 16:0	24:0; 22:0; 20:0; 26:0	15
928.9058	928.9055	0.30	C61 H118 04 N	2.09	18:1-d17:1/26:0	18:1;	25:0; 24:0; 17:1; 16:0; 16:1; 20:0; 20:1; 18:0; 26:0	24
930.9212	930.9212	0.00	C61 H120 04 N	17.21	18:0-d18:1/25:0	18:0;	24:0; 17:0; 19:0; 20:0; 16:0; 22:0; 23:0; 25:0; 21:0; 15:0; 26:0	33
942.9211	942.9212	−0.04	C62 H120 04 N	5.63	18:0-d18:1/26:1	18:0;	18:1; 20:0; 20:1; 22:0; 16:0; 24:0	18
944.9368	944.9368	−0.06	C62 H122 04 N	35.40	18:0-d18:1/26:0	18:0;	20:0; 24:0; 22:0; 16:0; 14:0; 26:0	18
956.9368	956.9368	−0.08	C63 H122 04 N	2.12	22:0-d17:1/24:1	22:0;	24:0; 18:1; 24:1; 20:1; 20:0; 21:0; 23:0; 19:1; 25:0; 25:1; 26:1; 26:0; 16:0; 16:1	40
958.9523	958.9525	−0.15	C63 H124 04 N	17.20	22;0-d18:1/23:0	22:0;	24:0; 20:0; 18:0; 23:0; 21:0;19:0; 16:0; 25:0; 17:0; 26:0; 15:0	35
970.9525	970.9525	0.04	C64 H124 04 N	6.40	22:0-d18:1/24:1; 22:1-d18:1/24:0	22:0; 22:1	24:1; 24:0; 18:0; 20:0; 20:1; 16:0; 26:1; 14:0; 30:1; 28:1	34
972.9680	972.9681	−0.10	C64 H126 04 N	48.40	22:0-d18:1/24:0; 24:0-d18:1/22:0	22:0; 24:0	20:0; 18:0; 23:0; 16:0	15
984.9681	984.9681	0.00	C65 H126 04 N	8.15	24:0-d17:1/24:1; 24:1-d17:1/24:0	24:0; 24:1	22:0; 25:0; 22:1; 23:1; 25:0; 25:1; 21:0; 26:1	33
986.9838	986.9838	0.03	C65 H128 04 N	48.45	24:0-d17:1/24:0	24:0;	22:0; 23:0; 21:0; 18:0; 25:0; 20:0; 16:0; 26:0; 17:0; 15:0	30
996.9679	996.9681	−0.19	C66 H126 04 N	2.28	24:0-d18:1/24:2; 24:1-d18:1/24:1	24:0; 24:1	24:2; 22:0; 22:1; 22:2; 26:1; 26:2; 20:1; 20:0; 25:0	24
998.9836	998.9838	−0.14	C66 H128 04 N	21.02	24:0-d18:1/24:1; 24:1-d18:1/24:0	24:0; 24:1	22:0; 16:0; 18:0; 26:0; 20:0; 32:0; 30:0; 28:0; 14:0	24
1,000.9994	1,000.9994	−0.07	C66 H130 04 N	100.00	24:0-d18:1/24:0	24:0;	22:0; 23:0; 25:0; 26:0	14
1,012.9993	1,012.9994	−0.11	C67 H130 04 N	13.23	24:0-d18:1/25:1; 24:0-d17:1/26:1; 24:1-d18:1/25:0	24:0; 24:1	23:0; 25:1; 25:0; 26:1; 22:0; 18:0; 16:0; 17:0; 15:0; 20:0; 21:0; 19:0	33
1,015.0150	1,015.0151	−0.11	C67 H132 04 N	58.83	24:0-d18:1/25:0; 24:0-d17:1/26:0	24:0;	23:0; 25:0; 22:0; 26:0; 18:0; 16:0; 20:0	20
1,027.0149	1,027.0151	−0.16	C68 H132 04 N	22.43	24:0-d18:1/26:1; 24:1-d18:1/26:0	24:0; 24:1	26:1; 18:0; 16:0; 22:0; 20:0	15
1,029.0308	1,029.0307	0.06	C68 H134 04 N	87.02	24:0-d18:1/26:0	24:0;	26:0; 21:0; 18:0	10
1,043.0457	1,043.0457	−0.08	C69 H136 04 N	10.52	25:0-d18:1/26:0; 24:0-d18:1/27:0; 26:0-d18:1/25:0	25:0,24:0, 26:0;	23:0; 22:0; 28:0; 27:0	20
1,053.0307	1,053.0307	−0.08	C70 H134 04 N	2.29	26:1-d18:1/26:1; 26:2-d 18:1/26:0	26:1; 26:2	24:0; 24:1; 26:0; 28:1; 24:2; 22:0; 28:2; 22:1; 28:0	27
1,055.0464	1,055.0464	0.04	C70 H136 04 N	5.14	26:1-d18:1/26:0; 24:0-d18:1/28:1	26:1; 24:0	26:0; 28:1; 25:0; 30:1; 27:1	21
1,057.0623	1,057.0620	0.23	C70 H138 04 N	9.11	26:0-d18:1/26:0; 24:0-d18:1/28:0	26:0; 24:0	22:0; 25:0; 28:0; 27:0; 30:0	18
Total								710

[a]Abundances in descending order.
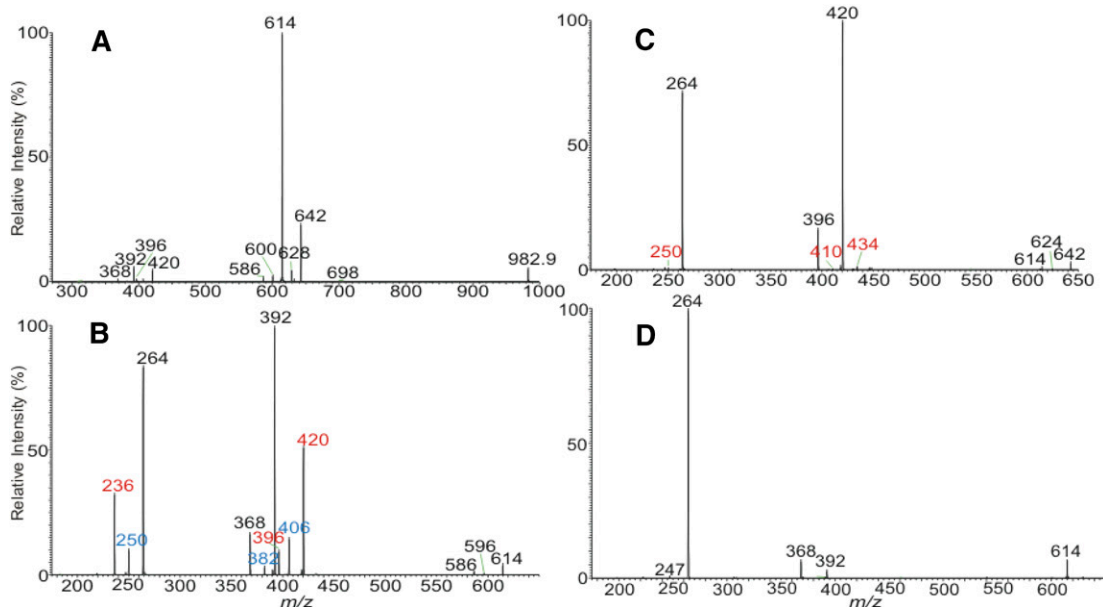[b]Detected in fraction 3.

Fig. 2. The MS[3] spectrum of the ions of m/z 982.9 (1,001.1 → 982.9) (A) originated from the ion species of m/z 1,001, its MS[4] spectra of the ions of m/z 614 (1,001.1 → 982.9 → 614) (B), and of m/z 642 (1,001.1 → 982.9 → 642) (C). The MS[4] spectrum of the ions of m/z 614 (650 → 632 → 614) originated from [M + H]$^+$ ions of d18:1/24:0-Cer at m/z 650 is shown in (D).

substituents, respectively. The MS[4] spectrum of the major ions of m/z 614 (888 → 870 → 614; data not shown) is nearly identical to that shown in Fig. 2B, signifying the molecule mainly consists of d18:1/24:0-Cer, along with minor d16:1/26:0- and d17:1/25:0-Cer moieties, resulting in the assignment of 16:0-d18:1/24:0-Cer major isomer, together with minor 16:0-d16:1/26:0-Cer and 16:0-d17:1/25:0-Cer. Similarly, further dissociation of the ions of m/z 502 (888 → 870 → 502; Fig. 4B) gives rise to the ion set of m/z 280 (c_{2a}), 256 (d_{1a}), and 264 ($e_{3b''}$) that identify the d18:1/16:0 moiety, and the assignment of 24:0-d18:1/16:0-Cer. The MS[4] spectrum of the ions of m/z 642 (888 → 870 → 642; data not shown) is similar to that shown in Fig. 2C that recognizes the main d18:1/26:0- and minor d17:1/27:0-Cer substituents, and results in the assignment of 14:0-d18:1/26:0- and 14:0-d17:1/27:0-Cer

isomers. Further MS[4] on the ions of m/z 586 (888 → 870 → 586; Fig. 4C) gives rise to the ions of m/z 392 (c_{2a}), 368 (d_{1a}), and 236 ($e_{3b''}$) arising from 18:0-d16:1/24:0-Cer; of m/z 364 (c_{2a}), 340 (d_{1a}), and 264 ($e_{3b''}$) arising from 18:0-d18:1/22:0; and of m/z 378 (c_{2a}), 354 (d_{1a}), and 250 ($e_{3b''}$) arising from the minor isomer of 18:0-d17:1/23:0-Cer. MS[4] on the ions of m/z 628, 600, 558, 530, 516, 488, and 474 reveals the LCB/N-acyl substituents of the molecule (supplemental Table S2). The combined structural information from MS^n (n = 2–4) reveals 26 isobaric isomers (supplemental Table S2) in which 16:0-d18:1/24:0 and 24:0-d18:1/16:0-Cer are dominant. The fragment ions from MS[4] (MH$^+$ → [MH$^+$ − H$_2$O] → [MH$^+$ − H$_2$O − 1-O-FA] and the representative Cer core structures found in this study are listed in **Table 3**. In total, an estimate of 710 species were found in this lipid family.

TABLE 2. Structures of the isobaric isomers deduced from MS^n on the ions of m/z 1001.1

| MS[3] (1,001.1 → 982.99)[a] | | MS[4] (1,001.1 → 982.99 → F2) | | | | |
| | | LCB | N-Acyl | | | |
Fragment Ions (F2)	1-O-Acyl Group (from loss of)	$e_{3b''}$	c_{2a}	d_{1a}	LCB/N-Acyl Moieties	Structural Assignment
642	22:0	264	420	396	d18:1/26:0	22:0-d18:1/26:0
		250	434	410	d17:1/27:0	22:0-d17:1/27:0
628	23:0	250	420	396	d17:1/26:0	23:0-d17:1/26:0
		264	406	382	d18:1/25:0	23:0-d18:1/25:0
		278	392	368	d19:1/24:0	23:0-d19:1/24:0
614[b]	24:0	264	392	368	d18:1/24:0	**24:0-d18:1/24:0**
		236	420	396	d16:1/26:0	24:0-d16:1/26:0
		250	406	382	d17:1/25:0	24:0-d17:1/25:0
600	25:0	250	392	368	d17:1/24:0	25:0-d17:1/24:0
		264	378	354	d18:1/23:0	25:0-d18:1/23:0
		236	406	382	d16:1/25:0	25:0-d16:1/25:0
586	26:0	236	392	368	d16:1/24:0	26:0-d16:1/24:0
		264	364	340	d18:1/22:0	26:0-d18:1/22:0
		250	378	354	d17:1/23:0	26:0-d17:1/23:0

The main isomer is indicated by boldface type.
[a] Ions of m/z 982.99 are due to loss of water from ions of m/z 1,001.1 via MS^2.
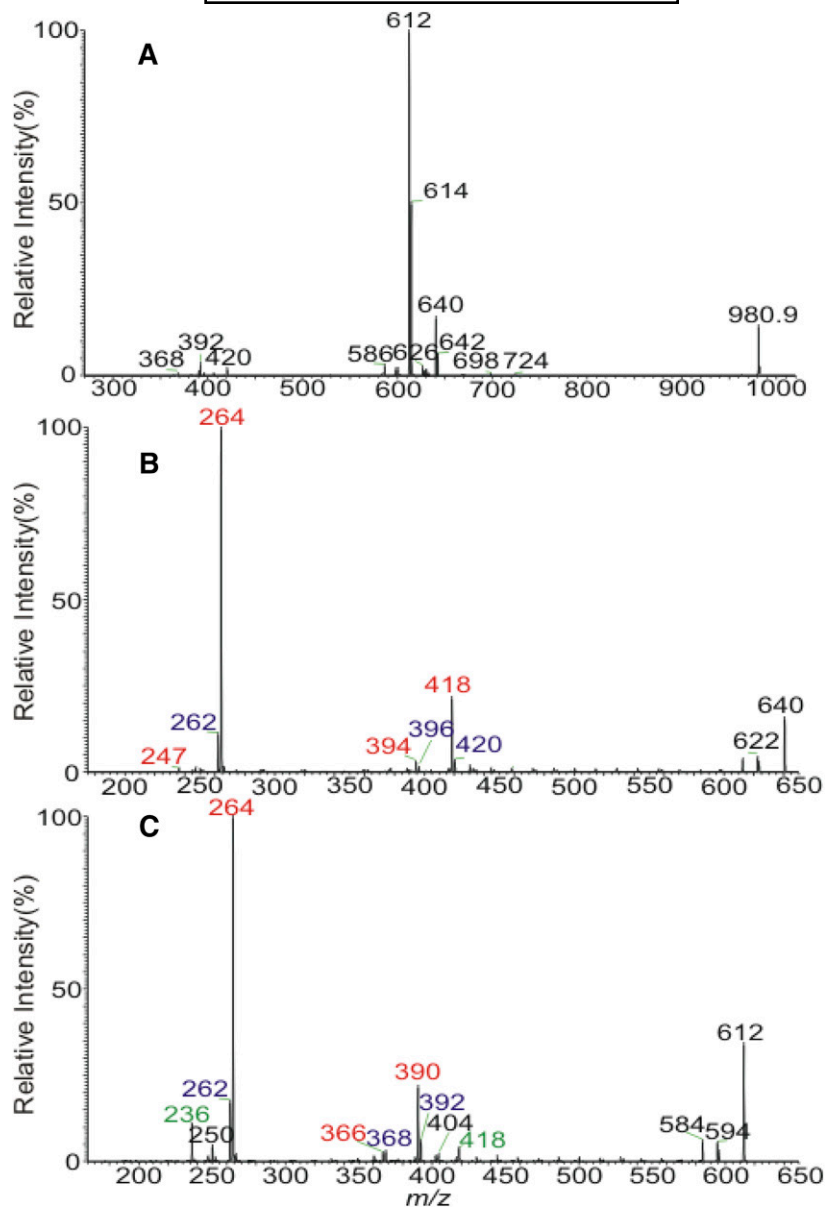[b] Major isomer.

Fig. 3. The MS^3 spectrum of the ion of m/z 980.9 (998.9 → 980.9) (A), its MS^4 spectra of the ions of m/z 640 (998.9 → 980.9 → 640) (B), and of m/z 612 (998.9 → 980.9 → 612) (C).

HCD tandem mass spectrometric analysis of FA-AMPP derivative for locating the double bond(s) on the fatty acyl chain

High-resolution mass measurements on the hydrolysate-AMPP reaction products revealed that the presence of the FA-AMPP ion series ranged from C14 to C32:0 with zero or one double bond (supplemental Table S3) in which the molecules with the saturated fatty acyl chain were the major species; while minor species with unsaturated bond and with odd chain acyl substituents were also present (supplemental Table S1). HCD MS^2 on the M$^+$ ions of the FA-AMPP derivatives indicated that the double bond position of the FA substituents were all located at n-9 (ω-9). For example, the HCD MS^2 spectrum of the ions of m/z 449 (see supplemental Fig. S1a) contained ions of m/z 349/351 and 295, 281, 253, 239, etc. together with major

ions of m/z 183 and 169 that are signature ions of the FA-AMPP derivative, showing that the double bond is located at n-9 and that the ion represents a $\Delta^9$18:1-FA (ω-9) (20, 22, 23). Another example is shown for the ions at m/z 533 (supplemental Fig. S1b), which yielded the analogous ions of m/z 433/435 and 379, 365, 351, etc., representing a Δ^{15}24:1-FA. Interestingly, the HCD MS^2 spectra of the ions of m/z 409 (supplemental Fig. S1c) and 421 (supplemental Fig. S1d) show that the species represent an anteoiso-15:0-FA and a $\Delta^6$16:1-FA, respectively.

DISCUSSION

It appears to be that the compositions of the Cer core with the same m/z in all the 1-O-acylceramide family are identical, regardless of the chain length or the unsaturation
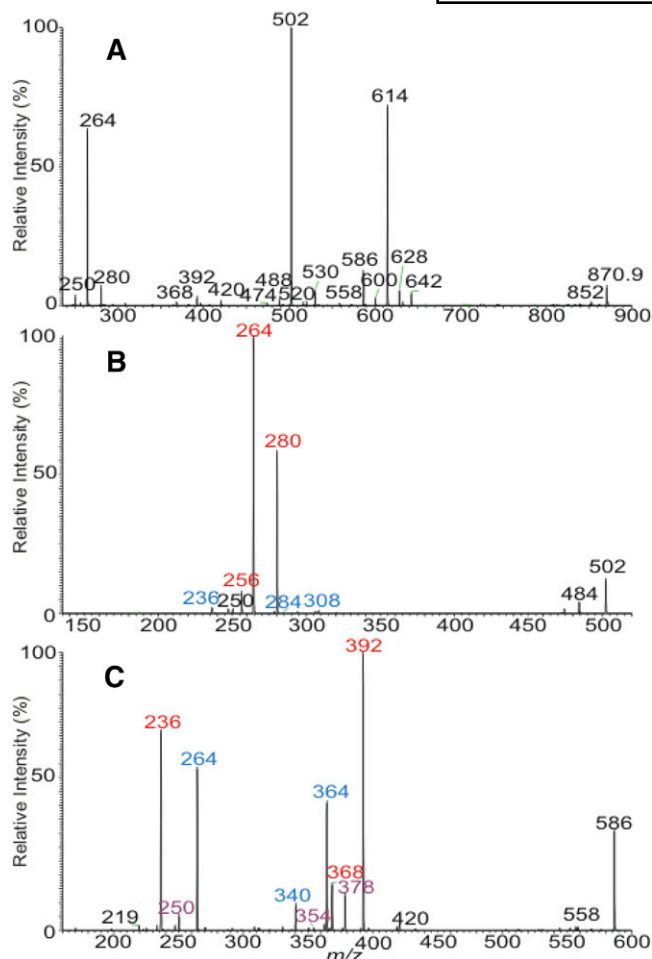
Fig. 4. The MS^3 spectrum of the ion of m/z 870.9 (888.9 → 870.9) (A), its MS^4 spectra of the ions of m/z 502 (888.9 → 870.9 → 502) (B) and of m/z 586 (888.9 → 870.9 → 586) (C).

status of the 1-O-acyl substituent. For example, the ions of m/z 642 arising from the MH$^+$ ions of m/z 1,001 by consecutive losses of water and 22:0-fatty acyl residues (Fig. 2C), of m/z 998.9 by the analogous losses of water and 1-O-22:1-FA residues (998.9 – water – 338), and of m/z 888.8 via losses of water and 1-O-14:0-FA (888.8 – water − 228) all consist of a major d18:1/26:0-Cer and a minor d17:1/27:0-Cer core structure; while ions of m/z 614 (Fig. 2B) represent mainly the d18:1/24:0-Cer and minor isomers of d16:1/26:0- and d17:1/25:0-Cer. These findings are consistent with the notion that the 1-O-acylceramide was synthesized from Cer by 1-O-acylation with the participation of diacylglycerol acyltransferase (6, 7). Another important finding in this study is that the abundant species, such as the ions of m/z 888.9, 916.9, 972.9, and 1,000.1, all contain d18:1/24:0-Cer as the major core structure, and the isobaric isomers are seen by the variation of the 1-O-acyl chain, rather than by variation of the Cer core. More than 20 isobaric isomers are present in more than half of the molecular species, and more than 700 structures (Table 1), including a minor subfamily consisting of dehydrosphingosine LCB, are present. Rabionet and colleagues (6, 7) reported the presence of the 1-O-acyl N-α-hydroxyacylceramide subfamily in mouse and human epidermis. Interestingly,

this Cer subfamily was found as a very minor species, and was eluted separately (fraction 3) from the major 1-O-acyl N-acylceramides (fraction 2). The presence of the vast number of structures in the 1-O-acylceramide family, as seen in this study, underscores the complexity of epidermal Cers, which consist of more than 10 Cer families (15, 16, 18, 24). Thus, this study highlights the utility of high-resolution LIT MS in the structural elucidation of complex lipid structures and the application of this technique in the complete characterization and differentiation of various Cer classes, including the location of the double bond(s) and hydroxyl group(s) on the fatty acyl chain and LCB has been reported recently (25).

There is a stark difference in the profiles of the MS^4 spectra of m/z 612 (Fig. 3C), of which the fatty acyl chain contains a double bond, and of m/z 614 (Fig. 2B), whose fatty acyl chain is saturated. The former spectrum is dominated by the ions of m/z 264 (e$_{3b''}$), and the ions of m/z 390 (c$_{2a}$) and 366 (d$_{1a}$) are of low abundance; while the ions of m/z 264 (e$_{3b''}$) in the MS^4 spectrum of the ions of m/z 614 are less prominent, and the analogous c$_{2a}$ ions at m/z 392 (Fig. 3C) and m/z 368 are abundant. The apparent differences in the MS^4 profiles were also observed for m/z 640 (Fig. 3B) and m/z 642 (Fig. 2C) pairs. Whether these differences in the abundances of the analogous fragment ions are attributable to the presence or absence of a double bond in the fatty acyl chain remains unclear. Interestingly, the MS^4 spectra of the ions of m/z 612 (648 → 630 →612) (data not shown) arising from the [M + H]$^+$ ions of d18:1/24:1-Cer (with a double bond in 24:1-FA substituent) and of m/z 614 (650 → 632 →614) (Fig. 2D) arising from the [M + H]$^+$ ions of d18:1/24:0-Cer (with no double bond in the 24:0-FA substituent) standards are all dominated by the ions of m/z 264, and the profiles of the spectra are similar to Fig. 3C, indicating that the fragmentation processes (supplemental Scheme S1) leading to the ion formation may be similar. The formation of the ions of m/z 612 (Fig. 3C) and m/z 614 (Fig. 2B) from 24:0-d18:1/24:1 and 24:0-d18:1/24:0-Cer, respectively, arising from the first loss of a water molecule may involve the participation of the 3-OH group of the LCB, followed by elimination of the 1-O-acyl group (Scheme 1). In contrast, the formation of the ions of m/z 612 (648 → 630 →612) originated from the [M + H]$^+$ ions of d18:1/24:1-Cer and of m/z 614 (650 → 632 → 614) originated from the [M + H]$^+$ ions of d18:1/24:0-Cer involves the consecutive losses of water, in which the first water loss may involve the participation of the 1-hydroxy group (supplemental Scheme S1). However, whether this difference in the sequence of the elimination processes leading to these precursor ions (i.e., the third generation ions) contributes to the differential cleavage of fatty acyl groups to form the ions of m/z 264 upon being further subjected to CID is also unclear. The prominence of the ions of m/z 264, as seen in Fig. 1C, may also reflect the fact that loss of a shorter 17:0-fatty acyl chain as a ketene in 18:1-d18:1/17:0-Cer is probably more facile than the analogous loss of the longer 26:0-fatty acyl chain in 22:0-d18:1/26:0-Cer, as supported by the notion that ions of m/z 264 in the MS^4 spectrum of m/z 642 (Fig. 2c) is less prominent (than m/z 420).

TABLE 3. The MS^4 [MH$^+$] → [MH$^+$ − H$_2$O] → [MH$^+$ − H$_2$O − 1-O-FA] fragment ions and the representative LCB/N-acyl strictures

Precursor ion (from MS^3) [MH$^+$ − H$_2$O − 1-O-FA]	LCB $e_{3b''}$	N-Acyl c_{2a}	d_{1a}	Structures (LCB/N-Acyl Moieties)
752	264	530	506	**d18:1/34:1**
738	250	530	506	**d17:1/34:1**
726	264	504	480	**d18:1/32:0**
724	264	502	478	**d18:1/32:1**
712	250	504	480	**d17:1/32:0**
698	264	476	452	**d18:1/30:0**
	250	490	466	d17:1/31:0[c]
696	264	474	452	**d18:1/30:1**
	236	502	478	d16:1/32:1[b]
694	262	474	450	**d18:2/30:1**
	236	502	478	d16:1/32:2[a]
684	264	462	438	**d18:1/29:0**
	250	476	452	d17:1/30:0[c]
	278	448	424	d19:1/28:0[b]
	306	420	396	d21:1/26:0[c]
670	264	448	424	**d18:1/28:0**
	292	420	396	d20:1/26:0[c]
668	264	446	422	**d18:1/28:1**
	236	474	450	d16:1/30:1[c]
	262	448	424	d18:2/28:0[c]
666	262	446	422	**d18:2/28:1**
	264	444	420	d18:1/28:2[a]
656	264	434	410	**d18:1/27:0**
	278	420	396	d19:1/26:0[b]
	250	448	424	d17:1/28:0[b]
654	264	432	408	**d18:1/27:1**
	250	446	422	d17:1/28:1[a]
	276	420	396	d19:2/26:0[b]
	278	418	394	d19:1/26:1[c]
642	264	420	396	**d18:1/26:0**
	250	434	410	d17:1/27:0[c]
640	264	418	394	**d18:1/26:1**
	262	420	396	d18:2/26:0[b]
	252	430	406	d17:0/27:2[c]
638	262	418	394	**d18:2/26:1**
	264	416	392	d18:1/26:2[a]
628	250	420	396	**d17:1/26:0**
	264	406	382	d18:1/25:0[b]
	236	434	410	d16:1/27:0[c]
626	250	418	394	**d17:1/26:1**
	264	404	380	d18:1/25:1[a]
	262	406	382	d18:2/25:0[b]
614	264	392	368	**d18:1/24:0**
	236	420	396	d16:1/26:0[a]
	250	406	382	d17:1/25:0[b]
612	264	390	366	**d18:1/24:1**
	262	392	368	d18:2/24:0[a]
	236	418	394	d16:1/26:1[b]
	250	404	380	d17:1/25:1[c]
610	264	388	364	**d18:1/24:2**
	262	390	366	**d18:2/24:1**
	250	402	378	d17:1/25:2[c]
600	250	392	368	**d17:1/24:0**
	264	378	354	d18:1/23:0[b]
	236	406	382	d16:1/25:0[b]
598	250	390	366	**d17:1/24:1**
	264	376	352	d18:1/23:1[c]
586	236	392	368	**d16:1/24:0**
	264	364	340	d18:1/22:0[c]
	250	378	354	d17:1/23:0[b]
584	264	362	338	**d18:1/22:1**
	262	364	340	d18:2/22:0[a]
	236	390	366	d16:1/24:1[a]
582	236	388	364	**d16:1/24:2**
572	250	364	340	**d17:1/22:0**
	264	350	326	d18:1/21:0[a]
	222	392	368	d15:1/24:0[a]
	236	378	354	d16:1/23:0[b]
	278	336	312	d19:1/20:0[b]

TABLE 3. Continued.

Precursor ion (from MS^3) [MH$^+$ − H$_2$O − 1-O-FA]	Fragment ions from MS^4			Structures (LCB/N-Acyl Moieties)
	LCB	N-Acyl		
	e$_{3b''}$	c$_{2a}$	d$_{1a}$	
570	250	362	338	**d17:1/22:1**
	264	348	324	d18:1/21:1[b]
	236	376	352	d16:1/23:1[c]
558	264	336	312	**d18:1/20:0**
	236	364	340	**d16:1/22:0**
	250	350	326	d17:1/21:0[b]
556	250	348	324	**d17:1/21:1**
544	264	322	298	**d18:1/19:0**
	250	336	312	d17:1/20:0[b]
530	264	308	284	**d18:1/18:1**
	278	294	270	d19:1/17:0[a]
	250	322	298	d17:1/19:0[c]
528	264	304	280	**d18:1/18:2**
526	264	304	280	**d18:1/18:2**
516	264	294	270	**d18:1/17:0**
514	250	306	282	**d17:1/18:1**
	264	292	268	d18:1/17:1[c]
512	250	304	280	**d17:1/18:2**
502	264	280	256	**d18:1/16:0**
500	264	278	254	**d18:1/16:1**
	236	306	282	d16:1/18:1
498	236	304	280	**d16:1/18:2**
488	250	280	256	**d17:1/16:0**
	264	266	242	d18:1/15:0[c]
474	236	280	256	**d16:1/16:0**
	264	252	228	d18:1/14:0[a]
	250	266	242	d17:1/15:0[c]
460	250	252	228	**d17:1/14:0**
	236	266	242	d16:1/15:0[c]

The main isomer (100%) is indicated by boldface type.
[a] Secondary isomer (<80%).
[b] Minor isomer (<50%).
[c] Trace isomer (<10%).

The observation of the 1-O-acyl and N-acyl substituents ranging from C14 to C32 with zero or one double bond in this Cer family (Table 1, 3) is consistent with the results from the high-resolution mass measurement of the AMPP derivatives of the acid hydrolysate that yielded the M$^+$ ion series ranging from C14 to C32 with zero or one double bond (supplemental Table S3). There are several minor species possessing two double bonds in the 1-O-acyl (e.g., 24:2 and 26:2; Table 1) or N-acyl (e.g., 24:2, 26:2, and 28:2; Table 3) chain, and the very long N-34:1-fatty acyl chain-containing species are also seen (Table 3). However, the corresponding FA species were not observed in the hydrolysate (supplemental Table S3). These FAs may be lost or too low to be detected after hydrolysis and derivatization steps. Nevertheless, the realization of the position of the double bond of the unsaturated FA substituents at n-9 for all the FA substituents, excepting 16:1-FA of which the double bond appears to be located at C6, is consistent with the notion of, for example, the presence of sphingolipids with d18:1/Δ^{15}24:1 (n-9) core structure as reported previously (26). The 16:1-FA appears to be a Δ^{6}16:1-FA, which is a sapienic acid exclusively found in sebum (27).

Results from our preliminary study indicate that there is a significantly higher abundance (greater than three times) of the 1-O-acylceramide family in the epidermis of FA transport protein 4 (FATP4)-deficient newborn mice (Fatp4$^{−/−}$ mice) compared with heterozygous control newborn mice (Fatp$^{+/−}$), while the level of the 1-O-acylceramide family is restored in the rescued null Fatp4 newborn mice (Fatp4$^{−/−}$; Tg(IVL-Fatp1) (28) (data not shown). Mutations in SLC27A4, the gene encoding FATP4, are known to cause ichthyosis prematurity syndrome in humans (29, 30). FATP4 is critical for development of fetal skin (31) and it has been hypothesized that lack of FATP4 in epidermal keratinocytes induces abnormal lipid metabolism in the epidermis that initiates the observed alterations in epidermal signaling pathways (32, 33). It is still unclear whether the FATP4 gene plays a role in the synthesis of this complex Cer family. Studies toward understanding the mechanism underlying the increase of this 1-O-acylceramide family in Fatp4 mutant fetal epidermis are currently in progress in our laboratory.

REFERENCES

1. Siegenthaler, U., A. Laine, and L. Polak. 1983. Studies on contact sensitivity to chromium in the guinea pig. The role of valence in the formation of the antigenic determinant. *J. Invest. Dermatol.* **80:** 44–47.
2. Imokawa, G., S. Akasaki, M. Hattori, and N. Yoshizuka. 1986. Selective recovery of deranged water-holding properties by stratum corneum lipids. *J. Invest. Dermatol.* **87:** 758–761.
3. Imokawa, G., S. Akasaki, Y. Minematsu, and M. Kawai. 1989. Importance of intercellular lipids in water-retention properties of

the stratum corneum: induction and recovery study of surfactant dry skin. *Arch. Dermatol. Res.* **281:** 45–51.

4. Wertz, P. W., and D. T. Downing. 1983. Ceramides of pig epidermis: structure determination. *J. Lipid Res.* **24:** 759–765.

5. Ponec, M., A. Weerheim, P. Lankhorst, and P. Wertz. 2003. New acylceramide in native and reconstructed epidermis. *J. Invest. Dermatol.* **120:** 581–588.

6. Rabionet, M., K. Gorgas, and R. Sandhoff. 2014. Ceramide synthesis in the epidermis. *Biochim. Biophys. Acta.* **1841:** 422–434.

7. Rabionet, M., A. Bayerle, C. Marsching, R. Jennemann, H-J. Gröne, Y. Yildiz, D. Wachten, W. Shaw, J. A. Shayman, and R. Sandhoff. 2013. 1-O-acylceramides are natural components of human and mouse epidermis. *J. Lipid Res.* **54:** 3312–3321.

8. Raith, K., J. Darius, and R. H. H. Neubert. 2000. Ceramide analysis utilizing gas chromatography–mass spectrometry. *J. Chromatogr. A.* **876:** 229–233.

9. Polito, A. J., T. Akita, and C. C. Sweeley. 1968. Gas chromatography and mass spectrometry of sphingolipid bases. Characterization of sphinga-4,14-dienine from plasma sphingomyelin. *Biochemistry.* **7:** 2609–2614.

10. Gu, M., J. L. Kerwin, J. D. Watts, and R. Aebersold. 1997. Ceramide profiling of complex lipid mixtures by electrospray ionization mass spectrometry. *Anal. Biochem.* **244:** 347–356.

11. Hsu, F-F., and J. Turk. 2002. Characterization of ceramides by low energy collisional-activated dissociation tandem mass spectrometry with negative-ion electrospray ionization. *J. Am. Soc. Mass Spectrom.* **13:** 558–570.

12. Hsu, F. F., J. Turk, M. E. Stewart, and D. T. Downing. 2002. Structural studies on ceramides as lithiated adducts by low energy collisional-activated dissociation tandem mass spectrometry with electrospray ionization. *J. Am. Soc. Mass Spectrom.* **13:** 680–695.

13. Sullards, M. C., and A. H. Merrill, Jr. 2001. Analysis of sphingosine 1-phosphate, ceramides, and other bioactive sphingolipids by high-performance liquid chromatography-tandem mass spectrometry. *Sci. STKE.* **2001:** pl1.

14. Han, X. 2002. Characterization and direct quantitation of ceramide molecular species from lipid extracts of biological samples by electrospray ionization tandem mass spectrometry. *Anal. Biochem.* **302:** 199–212.

15. Masukawa, Y., H. Narita, E. Shimizu, N. Kondo, Y. Sugai, T. Oba, R. Homma, J. Ishikawa, Y. Takagi, T. Kitahara, et al. 2008. Characterization of overall ceramide species in human stratum corneum. *J. Lipid Res.* **49:** 1466–1476.

16. t'Kindt, R., L. Jorge, E. Dumont, P. Couturon, F. David, P. Sandra, and K. Sandra. 2012. Profiling and characterizing skin ceramides using reversed-phase liquid chromatography-quadrupole time-of-flight mass spectrometry. *Anal. Chem.* **84:** 403–411.

17. Liebisch, G., W. Drobnik, M. Reil, B. Trümbach, R. Arnecke, B. Olgemöller, A. Roscher, and G. Schmitz. 1999. Quantitative measurement of different ceramide species from crude cellular extracts by electrospray ionization tandem mass spectrometry (ESI-MS/MS). *J. Lipid Res.* **40:** 1539–1546.

18. van Smeden, J., L. Hoppel, R. van der Heijden, T. Hankemeier, R. J. Vreeken, and J. A. Bouwstra. 2011. LC/MS analysis of stratum corneum lipids: ceramide profiling and discovery. *J. Lipid Res.* **52:** 1211–1221.

19. Robson, K. J., M. E. Stewart, S. Michelsen, N. D. Lazo, and D. T. Downing. 1994. 6-Hydroxy-4-sphingenine in human epidermal ceramides. *J. Lipid Res.* **35:** 2060–2068.

20. Hsu, F-F. 2016. Characterization of hydroxyphthioceranoic and phthioceranoic acids by charge-switch derivatization and CID tandem mass spectrometry. *J. Am. Soc. Mass Spectrom.* **27:** 622–632.

21. Hsu, F-F., K. Soehl, J. Turk, and A. Haas. 2011. Characterization of mycolic acids from the pathogen Rhodococcus equi by tandem mass spectrometry with electrospray ionization. *Anal. Biochem.* **409:** 112–122.

22. Yang, K., B. G. Dilthey, and R. W. Gross. 2013. Identification and quantitation of fatty acid double bond positional isomers: a shotgun lipidomics approach using charge-switch derivatization. *Anal. Chem.* **85:** 9742–9750.

23. Wang, M., R. H. Han, and X. Han. 2013. Fatty acidomics: global analysis of lipid species containing a carboxyl group with a charge-remote fragmentation-assisted approach. *Anal. Chem.* **85:** 9312–9320.

24. Kováčik, A., J. Roh, and K. Vávrová. 2014. The chemistry and biology of 6-hydroxyceramide, the youngest member of the human sphingolipid family. *ChemBioChem.* **15:** 1555–1562.

25. Hsu, F-F. 2016. Complete structural characterization of ceramides as [M-H]- ions by multiple-stage linear ion trap mass spectrometry. *Biochimie.* **130:** 63–75.

26. Poulos, A. 1995. Very long chain fatty acids in higher animals–a review. *Lipids.* **30:** 1–14.

27. Pappas, A. 2009. Epidermal surface lipids. *Dermatoendocrinol.* **1:** 72–76.

28. Lin, M. H., and D. Khnykin. 2014. Fatty acid transporters in skin development, function and disease. *Biochim. Biophys. Acta.* **1841:** 362–368.

29. Lin, M. H., and J. H. Miner. 2015. Fatty acid transport protein 1 can compensate for fatty acid transport protein 4 in the developing mouse epidermis. *J. Invest. Dermatol.* **135:** 462–470.

30. Klar, J., M. Schweiger, R. Zimmerman, R. Zechner, H. Li, H. Törmä, A. Vahlquist, B. Bouadjar, N. Dahl, and J. Fischer. 2009. Mutations in the fatty acid transport protein 4 gene cause the ichthyosis prematurity syndrome. *Am. J. Hum. Genet.* **85:** 248–253.

31. Gimeno, R. E., D. J. Hirsch, S. Punreddy, Y. Sun, A. M. Ortegon, H. Wu, T. Daniels, A. Stricker-Krongrad, H. F. Lodish, and A. Stahl. 2003. Targeted deletion of fatty acid transport protein-4 results in early embryonic lethality. *J. Biol. Chem.* **278:** 49512–49516.

32. Lin, M-H., F-F. Hsu, and J. H. Miner. 2013. Requirement of fatty acid transport protein 4 for development, maturation, and function of sebaceous glands in a mouse model of ichthyosis prematurity syndrome. *J. Biol. Chem.* **288:** 3964–3976.

33. Moulson, C. L., D. R. Martin, J. J. Lugus, J. E. Schaffer, A. C. Lind, and J. H. Miner. 2003. Cloning of wrinkle-free, a previously uncharacterized mouse mutation, reveals crucial roles for fatty acid transport protein 4 in skin and hair development. *Proc. Natl. Acad. Sci. USA.* **100:** 5274–5279.